WEB OF SCIENTIST: INTERNATIONAL SCIENTIFIC RESEARCH JOURNAL
ISSN: 2776-0979, Volume 3, Issue 6, June, 2022

STUDY OF ELECTROMAGNETIC PHENOMENA AND ITS MAIN PARAMETERS IN THE CRUCIBLE OF INDUCTION FURNACES DURING SMELTING STEEL 20GL

Tursunov Tokhir Muratovich
Senior Lecturer, of the Department of Materials Science and Mechanical Engineering, Tashkent State Transport University, Tashkent, The Republic of Uzbekistan
e-mail: t.tursunov87@gmail.com

Tursunov Nodirjon Kayumjonovich
Ph.D., Head of the Department of Materials Science and Mechanical Engineering, Tashkent State Transport University, Tashkent, The Republic of Uzbekistan,
e-mail: u_nadir@mail.ru

Urazbaev Talgat Tileubaevich
Senior Lecturer, of the Department of Materials Science and Mechanical Engineering, Tashkent State Transport University, Tashkent, The Republic of Uzbekistan

Alimukhamedov Shavkat Pirmukhamedovich
Dr. Tech. Sciences, Professor of the Department of Materials Science and Mechanical Engineering, Tashkent State Transport University, Tashkent, The Republic of Uzbekistan

Toirov Otabek Toir ugli
Ph.D. student of the Department of Materials Science and Mechanical Engineering, Tashkent State Transport University, Tashkent, The Republic of Uzbekistan

Abstract

This article is devoted to the study of electromagnetic phenomena in induction furnaces for smelting steel. The main objectives of this article are to study electromagnetic phenomena in liquid metal in a crucible to estimate electrical losses in an inductor, as well as to obtain calculation formulas for active power $P_м$ released in liquid steel, and reactive power $Q_м$ arising in liquid steel.

WEB OF SCIENTIST: INTERNATIONAL SCIENTIFIC RESEARCH JOURNAL
ISSN: 2776-0979, Volume 3, Issue 6, June, 2022

The listed parameters are necessary to calculate the optimal thickness of the lining of induction furnaces in order to increase the service life of the lining and increase the number of heats.

In the article were used: the mathematical expression of the solution of the equation through the complex functions $J_\vartheta(x)$ is represented by a graphical interpretation (obtained on the basis of a calculation using the IN program); Euler - Bessel equation; complex form of the Poynting vector S_R; incidence of a cylindrical electromagnetic wave on a solid metal cylinder with a diameter of $D_м$ for crucible of induction furnaces (ICF-6).

Keywords: electromagnetic wave, magnetic field strength, electric field strength, cylindrical wave, Poynting vector, active power, reactive power, coefficients

1. Introduction

This article is devoted to the study of electromagnetic phenomena in 6 ton induction furnaces when smelting steel grade 20GL (analogue for EU=G21Mn5 and USA = A352GrLCC) in the Subsidiary Foundry Mechanical Plant (FMP) in Tashkent. To study electromagnetic phenomena in a liquid metal in a crucible to estimate electrical losses in an inductor, it is necessary to use the rotor of the magnetic (1) and electric (2) field strengths in cylindrical coordinates. [4,2]

During most of the melting process, exactly from the moment when a part of the steel charge is melted, in which the still unmelted pieces can be accommodated, the steel charge is represented as a solid cylindrical block with $\mu_r = 1$. Steel satisfies this condition at temperatures above the Curie point. Therefore, the induction crucible furnace (ICF) is a cylindrical system "inductor - metal" (Fig. 1): the vector of the magnetic field strength is directed parallel to the axis of the cylindrical wave ($H = H_z;\ H_\psi = 0;\ H_R = 0$); the vector of the electric field strength is directed tangentially to the circles, the centers of which lie on the axis of the cylindrical inductor ($E = E_\psi;\ E_z = 0;\ E_R = 0$) [2,4] .

WEB OF SCIENTIST: INTERNATIONAL SCIENTIFIC RESEARCH JOURNAL
ISSN: 2776-0979, Volume 3, Issue 6, June, 2022

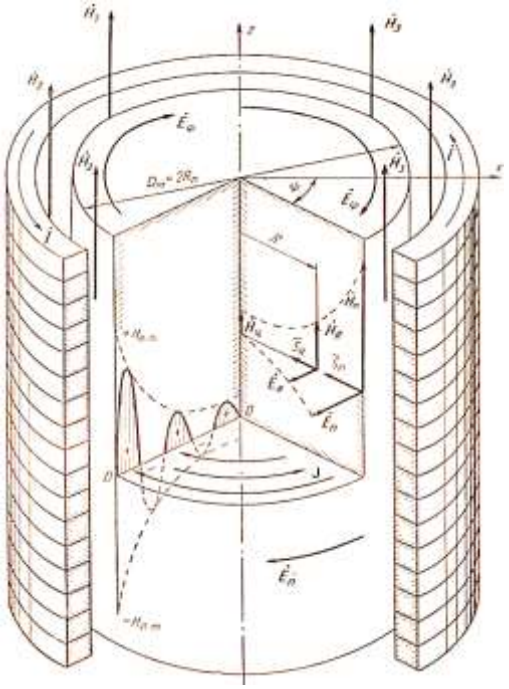

Figure 1 – The incidence of a cylindrical electromagnetic wave on a solid metal

cylinder with a diameter $D_м$ (for ICF -6 in FMP $D_м = 1050$ mm):
I - current in the inductor; $H_з$, $H_п$, H_R и $H_ц$ - magnetic field strength in the gap, on the surface, at a point with radius R and on the axis of the metal cylinder, respectively; $E_п$ и E_R – the electric field strength on the surface and at a point with a radius R; ψ - meridian angle (longitude); the O-O axis shows the diagram of the instantaneous values of the magnetic field strength; arrows indicate the direction of the corresponding electric lines of force (line of conduction currents J) along the cross-section of the cylinder [2]

2. Methods

In cylindrical coordinates, the rotor of the magnetic (1) and electric (2) field strengths can be solved, respectively,
through the determinant

$$[\nabla H] = \begin{vmatrix} 1_R & 1_\psi & 1_z \\ \frac{\partial}{\partial R} & \frac{\partial}{\partial \psi} & \frac{\partial}{\partial z} \\ H_R & H_\psi & H_z \end{vmatrix} = 1_R \frac{\partial}{\partial \psi} H_z + 1_\psi \frac{\partial}{\partial z} H_R + 1_z \frac{\partial}{\partial R} H_\psi - 1_R \frac{\partial}{\partial z} H_\psi - 1_\psi \frac{\partial}{\partial R} H_z - 1_z \frac{\partial}{\partial \psi} H_R. \quad (1)$$

WEB OF SCIENTIST: INTERNATIONAL SCIENTIFIC RESEARCH JOURNAL
ISSN: 2776-0979, Volume 3, Issue 6, June, 2022

$$[\nabla E] = \begin{vmatrix} 1_R & 1_\psi & 1_z \\ \frac{\partial}{\partial R} & \frac{\partial}{\partial \psi} & \frac{\partial}{\partial z} \\ E_R & E_\psi & E_z \end{vmatrix} = 1_R \frac{\partial}{\partial \psi} E_z + 1_\psi \frac{\partial}{\partial z} E_R + 1_z \frac{\partial}{\partial R} E_\psi - 1_R \frac{\partial}{\partial z} E_\psi - 1_\psi \frac{\partial}{\partial R} E_z - 1_z \frac{\partial}{\partial \psi} E_R. \quad (2)$$

After transformations received:

$$\nabla^2 H_z = \frac{\partial^2 H_z}{\partial R^2} + \frac{1}{R}\frac{\partial H_z}{\partial R};$$

$$\nabla^2 E_\psi = \nabla^2 E_\psi - \frac{1}{R^2} E_\psi = \frac{\partial^2 E_\psi}{\partial R^2} + \frac{1}{R}\frac{\partial E_\psi}{\partial R} - \frac{1}{R^2} E_\psi.$$

Vector Laplacians for the magnetic intensity vector H_z field and vector of electric field strength E_ψ at a distance R for a conductive medium:

$$\frac{\partial^2 H_z}{\partial R^2} + \frac{1}{R} \cdot \frac{\partial H_z}{\partial R} = \frac{j\omega \mu_{абс} H_z}{\rho_м}; \quad (3)$$

$$\frac{\partial^2 E_\psi}{\partial R^2} + \frac{1}{R} \cdot \frac{\partial E_\psi}{\partial R} - \frac{1}{R^2} \cdot E_\psi = \frac{j\omega \mu_{абс} E_\psi}{\rho_м}. \quad (4)$$

Considering that

$$-\frac{j\omega \mu_{абс}}{\rho_м} = \left(j^{\frac{3}{2}} \cdot \frac{\sqrt{2}}{\delta_{eqv}}\right)^2, \quad (5)$$

Eqs. (3) and (4) can be given a simpler form by substituting the complex variable instead of the only independent variable R $\xi = \left(j^{\frac{3}{2}} \cdot \frac{\sqrt{2}R}{\delta_{eqv}}\right)^2$ and replace partial derivatives with ordinary ones (since H_z and E_ψ are functions of the only variable):

$$\frac{\partial^2 H_z}{\partial \xi^2} + \frac{1}{\xi} \cdot \frac{\partial H_z}{\partial \xi} + H_z = 0; \quad (6a)$$

$$\frac{\partial^2 E_\psi}{\partial \xi^2} + \frac{1}{\xi} \cdot \frac{\partial E_\psi}{\partial \xi} + \left(1 - \frac{1}{\xi^2}\right) \cdot E_\psi = 0. \quad (6b)$$

WEB OF SCIENTIST: INTERNATIONAL SCIENTIFIC RESEARCH JOURNAL
ISSN: 2776-0979, Volume 3, Issue 6, June, 2022

Equations (6a) and (6b) represent special cases of a homogeneous linear differential equation of the second order with the index ϑ (the so-called Euler - Bessel equation):

$$\frac{\partial^2 y}{\partial x^2} + \frac{1}{x} \cdot \frac{\partial y}{\partial x} + \left(1 - \frac{\vartheta^2}{x^2}\right) \cdot y = 0. \quad (7)$$

i.e., equation (6a) is an equation with the index ϑ = 0, equation (6b) - with the index ϑ = 1. Their solutions are represented as a linear combination of a cylindrical function of the first kind $J_\vartheta(x)$ and a cylindrical function of the third kind of the second kind $H_\vartheta^{(2)}(x)$:

$$y = A_\vartheta J_\vartheta(x) + C_\vartheta H_\vartheta^{(2)}(x). \quad (8)$$

Given the nature of the change in function J_ϑ and $H_\vartheta^{(2)}$ on the complex variable ξ, we can say that the first term in expression (8) describes the incident wave propagating from the cylinder surface to its axis, and the second term describes the reflected wave propagating from the cylinder axis to the surface. A solid cylinder has no reflective surfaces, so there will be no reflected wave, i.e. the constant of integration C_ϑ is equal to zero.

3. Results and Discussion

The mathematical expression of the solution to equation (8) in terms of complex functions $J_\vartheta(x)$ is represented by a graphical interpretation equations of magnetic and electric fields in a liquid metal in the form of the dependence of the relative modulus of complex vectors of intensity:
magnetic field

$$|H|_* = \frac{|H_z|}{|H_\Pi|} = \varphi'\left(\frac{R}{R_\Pi}\right). \quad (9)$$

and electric field strength

$$|E|_* = \frac{|E_\psi|}{|E_\Pi|} = \varphi''\left(\frac{R}{R_\Pi}\right). \quad (10)$$

and, which is the same, the complex vector of the conduction current density

$$|J|_* = \frac{|J_\psi|}{|J_\Pi|} = \varphi''\left(\frac{R}{R_\Pi}\right).. \quad (11)$$

WEB OF SCIENTIST: INTERNATIONAL SCIENTIFIC RESEARCH JOURNAL
ISSN: 2776-0979, Volume 3, Issue 6, June, 2022

on the relative volume radius of 20ГЛ (analogue for EU=G21Mn5 and USA = A352GrLCC) liquid steel in the ICF-6 crucible $R_* = R/R_п$. It should be borne in mind that the value $R_* = 0$ corresponds to the crucible axis, a $R_* = 1$ - inner surface of the crucible.

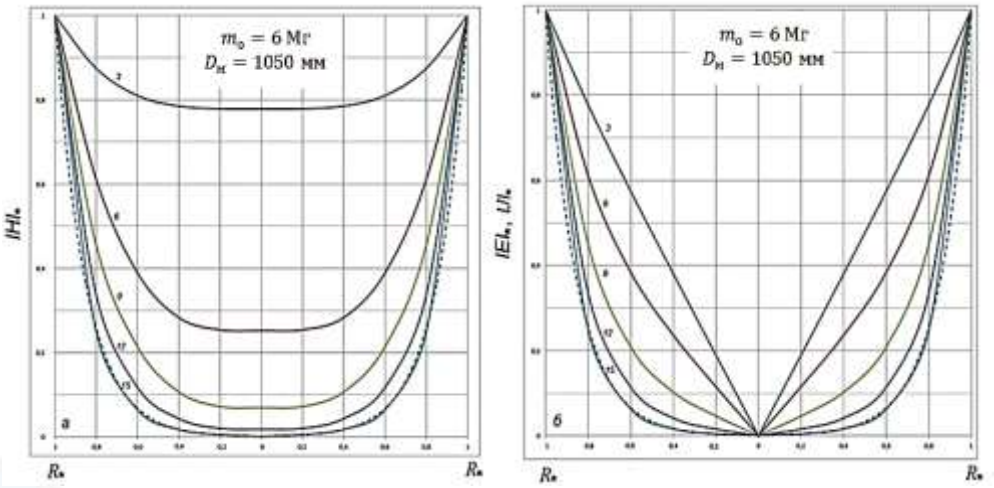

Figure 2 – Distribution of the relative modulus of the complex vectors of the magnetic field strength $|H|_*$ (a), electric field strength $|E|_*$ and conduction current density $|J|_*$ (б) in liquid metal ICF-6 ($D_м = 1050$ mm) (numbers near curves – values $D_м/\delta_{eqv}$; - exponent built for $D_м/\delta_{eqv} = 15$)

Argument values $D_м/\delta_{eqv}$ (see Fig. 1) for each curve correspond to the frequency (table № 1) according to the formula

$$f = \frac{500^2 \rho_м}{\mu_r \delta_{eqv}^2} = \frac{0.35}{\delta_{eqv}^2},$$

where $\rho_м = 140 \cdot 10^{-8}$ Om·m – for liquid steel brands 20ГЛ ($\mu_r = 1$);
$D_м = 1050$ mm $= 1.05$ m.

Based on the results of numeric values $D_м/\delta_{eqv}$ the curves (see Fig. 2) correspond to the values of the current frequency f (table № 1).

Table 1-Results of calculating compliance

$D_м/\delta_{eqv}$	3	6	9	12	15
f, Hz	2.9	11.4	25.7	45.7	71.4

WEB OF SCIENTIST: INTERNATIONAL SCIENTIFIC RESEARCH JOURNAL
ISSN: 2776-0979, Volume 3, Issue 6, June, 2022

Based on the results of numeric values $\frac{D_м}{\delta_{eqv}}$ the curves (Fig. 2) correspond to the values of the metal diameter in the crucible $D_м$ (table № 2).

Table 2- Results of calculating compliance

$D_м/\delta_{eqv}$	3	6	9	12	15
$D_м$, мм	114	227	340	453	567

A cylindrical wave carries electromagnetic energy determined by the vector of energy flux density per unit time S_R. In complex form, the Poynting vector S_R is the vector product of the complex of the electric field strength E_ψ by the conjugate complex of the magnetic field strength H_z

$$S_R = 0.5\left[E_\psi H_z^*\right]. \quad (12)$$

The scalar expression for the complex value of the power flux through the side surface of a metal cylinder with a diameter $D_м$, which is numerically equal to the lateral surface area S_{act} , allows one to obtain calculation formulas for the active power $P_м$ (15) according to (13), released in liquid steel, and the reactive power $Q_м$ (16), according to (14) arising in liquid steel [4]:

a) active power flux density, characterizing the rate of conversion of electromagnetic field energy into heat, kW/m²:

$$ReS = q_{act} \approx 2 \cdot 10^{-6}(IN_1)^2\sqrt{\rho_m \cdot \mu_r \cdot f}, \quad (13)$$

where $2 \cdot 10^{-6} \approx \frac{2\pi \cdot 10^{-6}}{\sqrt{10}}$;

$(IN_1) = \frac{IN}{h_и}$ - flooring of the inductor current, which determines the magnitude of the magnetic field strength on the inner surface and in the cavity of the inductor, $\frac{A}{m}$.

b) the reactive power flux density, which characterizes the rate of conversion of the energy of the electromagnetic field from an electric form to a magnetic form and vice versa, kW/m²:

$$ImS = q_{reactive} \approx 2 \cdot 10^{-6}(IN_1)^2\sqrt{\rho_м \cdot \mu_r \cdot f}. \quad (14)$$

$$P_м = ReS \cdot S_{act}k_{мP} \approx 2 \cdot 10^{-6}(IN_1)^2\pi D_м h_м\sqrt{\rho_м \mu_{rм}}fk_{мP} \approx$$
$$\approx 6.28 \cdot 10^{-6}(IN_1)^2 D_м h_м\sqrt{\rho_м}fk_{мP} = 2.4 \cdot 10^{-7}(IN_1)^2 k_{мP}, \ kW; \quad (15)$$

$$Q_м = Im\, S \cdot S_{act}k_{мQ} \approx 2 \cdot 10^{-6}(IN_1)^2\pi D_м h_м\sqrt{\rho_м \mu_{rм}}fk_{мQ} \quad (16)$$

WEB OF SCIENTIST: INTERNATIONAL SCIENTIFIC RESEARCH JOURNAL
ISSN: 2776-0979, Volume 3, Issue 6, June, 2022

$$Q_м = 6.28 \cdot 10^{-6}(IN_1)^2 D_м h_м \sqrt{\rho_м f} k_{мQ} = 1.92 \cdot 10^{-7}(IN_1)^2 k_{мQ},$$ kW.

where $\rho_м = 140 \cdot 10^{-8}$ Om·m – for liquid steel brands 20ГЛ ($\mu_r = 1$);

$S_{act} = \pi D_м h_м \approx 4.53$ m^2 – the area of the side ("active") surface of the heated volume of liquid metal in the ICF crucible with a diameter $D_м = 1.05$ m и height $h_м = 1.375$ m;

$2 \cdot 10^{-6} \approx \frac{2\pi \cdot 10^{-6}}{\sqrt{10}}$ – coefficient;

$6.28 \cdot 10^{-6} \approx 2\pi \cdot 10^{-6}$ – coefficient;

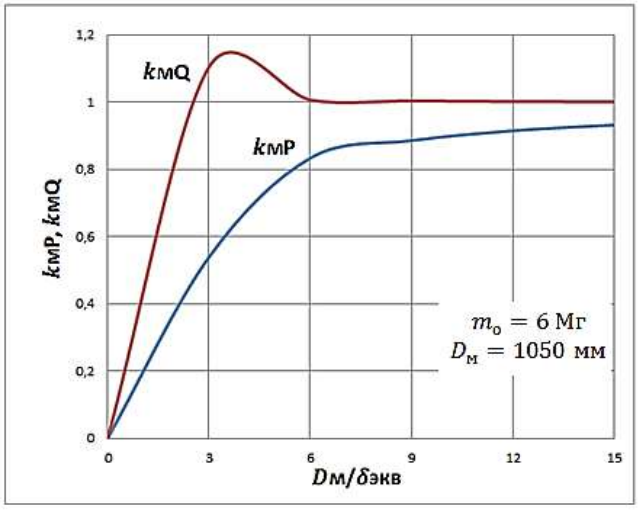

Figure 3 - Curves for determining the coefficients of active and reactive power

$k_{мP}, k_{мQ}$ - active and reactive power coefficients, respectively, taking into account the peculiarities of the physical processes of propagation and attenuation of cylindrical electromagnetic waves in the liquid metal ICF-6 and depending on the relative diameter of the cylinder $D_м/\delta_{eqv}$.

References

1. Семин, А. Е., Турсунов, Н. К., & Косырев, К. Л. (2017). Инновационное производство высоколегированной стали и сплавов. Теория и технология выплавки стали в индукционных печах.
2. Турсунов, Н. К., Семин, А. Е., & Саидирахимов, А. А. (2017). Теоретический и экспериментальный анализ процесса перевода индукционной тигельной печи из разряда переплавной установки в активный рафинирующий сталеплавильный агрегат. In Физико-химические основы металлургических процессов (pp. 62-62).
3. Ablyalimov, O. S. (2016). Concerning the efficiency of 3VL80S electromotives used on a hilly and mountainous railway section/OS Abljalimov, ZZ Ergashev, TM

Tursunov. In II international scientific and practical conference «Increase of energetic efficiency of ground-based transport systems»/Omsk state railway university. Omsk (pp. 105-111).

4. Ablyalimov, O. S. (2017). To the analysis of the transportation work of UzTE16M3 diesel locomotives in the hilly-mountainous section of the railway track/OS Ablylimov, TM Tursunov, MI Khismatulin. Vestnik TashIIT, (4), 57-61.
5. Ablyalimov, O. S. (2016). Concerning the efficiency of 3VL80S electromotives used on a hilly and mountainous railway section/OS Abljalimov, ZZ Ergashev, TM Tursunov. In II international scientific and practical conference «Increase of energetic efficiency of ground-based transport systems»/Omsk state railway university. Omsk (pp. 105-111).
6. Аблялимов, О. С., Турсунов, Т. М., & Салимов, Ф. А. (2015). К анализу использования магистральных грузовых электровозов «Узбекистан» на горном участке железной дороги. Вестник ТашИИТ, (3-4), 48.
7. Турсунов, Н. К., Уразбаев, Т. Т., & Турсунов, Т. М. (2022). Методика расчета комплексного раскисления стали марки 20гл с алюминием и кальцием. Universum: технические науки, (2-2 (95)), 20-25.
8. Makhkamov, N. Y., Yusupov, G. U., Tursunov, T., & Djalilov, K. (2020, December). Properties of metal-based and nonmetal-based composite materials: A brief review. In IOP Conference Series: Earth and Environmental Science (Vol. 614, No. 1, p. 012068). IOP Publishing.
9. Турсунов, Н. К., Турсунов, Т. М., & Уразбаев, Т. Т. (2022). Оптимизация футеровки индукционных печей при выплавке стали марки 20ГЛ. Обзор. Universum: технические науки, (2-2 (95)), 13-19.
10. Аблялимов, О. С., Ергашев, З. З., & Турсунов, Т. М. (2016). К эффективности использования электровозов 3ВЛ80С на холмисто-горном участке железной дороги. In Повышение энергетической эффективности наземных транспортных систем (pp. 105-111).
11. Аблялимов, О. С., Турсунов, Т. М., & Хисматулин, М. И. (2017). К анализу перевозочной работы тепловозов UzTE16M3 на холмисто-горном участке железнодорожного пути. Вестник ТашИИТ»/Ташкентский ин-т инж. ж.-д. транспорта, (4), 57-61.
12. Уразбаев, Т. Т., & Зайнитдинов, О. И. (2020). Повышение механических свойств боковой рамы двухосной тележки грузовых вагонов. Вестник транспорта Поволжья, (1), 27-34.
13. Fayzibaev, S. S., Soboleva, I. Y., Zainidinov, O. I., Urazbaev, T. T., & Samborskaya, N. A. (2019). To the question of the formation of composite compounds of the

system (Ti-Al). Slovak international scientific journal, 1(29), 5782.

14. Желудкевич, А. Л., Паршутич, С. Ф., Файзибаев, Ш. С., Уразбаев, Т. Т., & Игнатенко, О. В. (2021). Разработка связки на основе соединений системы Ti-Al для композиционного инструментального материала NB-Ti-Al. In Порошковая металлургия: инженерия поверхности, новые порошковые композиционные материалы. Сварка (pp. 399-407).
15. Файзибаев, Ш. С., Нигай, Р. П., Самборская, Н. А., Уразбаев, Т. Т., & Нафасов, Ж. Х. У. (2021). Режущий композиционный инструментальный материал на основе связки соединения системы bn-ti-al для чистовой обточки железнодорожных деталей. Universum: технические науки, (3-1 (84)), 82-87.
16. Alimukhamedov, S. P., Abdukarimov, A., Sharifhodjaeva, H. A., & Rustamov, K. J. (2020). Structural and kinematic analysis of gear and lever differential mechanisms by symmetric movement of rotation centers for driving and slave gear wheels. International Journal of Psychosocial Rehabilitation, 24(01).
17. Мухитдинов, А. А., & Алимухаммедов, Ш. П. Методическое указание к выполнению диссертационной работы на соискание ученной степени кандидата технических наук.
18. Алимухамедов, Ш. П., & Гапиров, А. Д. (2018). Напряженно-деформированное состояние устройства для гашения динамических нагрузок в трансмиссии транспортных машин. Universum: технические науки, (12 (57)), 23-28.
19. Алимухамедов, Ш. П., Рахимов, Р. В., Инагамов, С. Г., Мамаев, Ш. И., & Кодиров, Н. С. (2022). Математическое моделирование передаточного механизма потележечной тормозной системы грузовых вагонов. Universum: технические науки, (2-3 (95)), 8-14.
20. Akhmedov, D., Alimukhamedov, S., Tursunov, I., Narziev, S., & Riskaliev, D. (2021). Modeling the steering wheel influence by the driver on the vehicle's motion stability. In E3S Web of Conferences (Vol. 264). EDP Sciences.
21. Tursunov, N. K., Toirov, O. T., Nurmetov, K. I., Azimov, S. J., & Qo'Chqorov, L. A. (2022). Development of innovative technology of the high-quality steel production for the railway rolling stock cast parts. Oriental renaissance: Innovative, educational, natural and social sciences, 2(Special Issue 4-2), 992-997.
22. Турсунов, Н. К., Авдеева, А. Н., Мамаев, Ш. И., & Нигматова, Д. И. (2022). Метрология и стандартизация: роль и место дисциплины в подготовке специалистов железнодорожного транспорта республики узбекистан. Academic research in educational sciences, 3(TSTU Conference 1), 140-145.

23. Tursunov, N. K., Toirov, O. T., Nurmetov, K. I., & Azimov, S. J. (2022). Improvement of technology for producing cast parts of rolling stock by reducing the fracture of large steel castings. Oriental renaissance: Innovative, educational, natural and social sciences, 2(Special Issue 4-2), 948-953.
24. Азимов, Ё. Х., Рахимов, У. Т., Турсунов, Н. К., & Тоиров, О. Т. (2022). Исследование влияние катионов солей на реологический статус гелланової камеди до гелеобразования. Oriental renaissance: Innovative, educational, natural and social sciences, 2(Special Issue 4-2), 1010-1017.
25. Risqulov, A. A., Sharifxodjayeva, X. A., Tursunov, N. Q., & Nurmetov, X. I. (2022). Transport sohasi uchun mutaxassislarni tayyorlashda materialshunoslik yo ‘nalishining o‘rni va ahamiyati. Academic research in educational sciences, 3(TSTU Conference 1), 107-112.
26. Тоиров, О. Т. У., Турсунов, Н. К., & Кучкоров, Л. А. У. (2022). Совершенствование технологии внепечной обработки стали с целью повышения ее механических свойств. Universum: технические науки, (4-2 (97)), 65-68.
27. Туракулов, М. Р., Турсунов, Н. К., & Инсапов, Д. М. (2022). Разработка технологии изготовления формовочных и стержневых смесей для получения синтетического чугуна. Universum: технические науки, (4-3 (97)), 5-9.
28. Нурметов, Х. И., Турсунов, Н. К., Туракулов, М. Р., & Рахимов, У. Т. (2021). Усовершенствование материала конструкции корпуса автомобильной тормозной камеры. Scientific progress, 2(2), 1480-1484.
29. Toirov, O. T., Tursunov, N. Q., Nigmatova, D. I., & Qo’chqorov, L. A. (2022). Using of exothermic inserts in the large steel castings production of a particularly. Web of Scientist: International Scientific Research Journal, 3(1), 250-256.
30. Турсунов, Н. К., Тоиров, О. Т., Железняков, А. А., & Комиссаров, В. В. (2021). Снижение дефектности крупных литых деталей подвижного состава железнодорожного транспорта за счет выполнения мощных упрочняющих рёбер.
31. Нурметов, Х. И., Турсунов, Н. К., Кенжаев, С. Н., & Рахимов, У. Т. (2021). Перспективные материалы для механизмов автомобильных агрегатов. Scientific progress, 2(2), 1473-1479.
32. Тоиров, О. Т., Турсунов, Н. К., Кучкоров, Л. А., & Рахимов, У. Т. (2021). Исследование причин образования трещины в одной из половин стеклоформы после её окончательного изготовления. Scientific progress, 2(2), 1485-1487.